Ligand Binding, Conformational and Spectroscopic Properties, and Biomimetic Monooxygenase Activity by the Trinuclear Copper–PHI Complex Derived from L-Histidine

Michele Gullotti,[a] Laura Santagostini,[a] Roberto Pagliarin,[b] Sara Palavicini,[c] Luigi Casella,*[c] Enrico Monzani,[c] and Giorgio Zoppellaro[d]

The trinuclear copper(II) complex derived from the octadentate N-donor ligand PHI [piperazine-1,4-bis(4-{N-[1-acetoxy-3-(1-methyl-1H-imidazol-4-yl)]-2-propyl}-N-(1-methyl-1H-imidazol-2-ylmethyl)aminobutyl)] contains two equivalent Cu_A centers bound by tridentate arms and a Cu_B center bound by a central didentate residue. The conformational and ligand binding properties of the complex were extensively studied by various spectroscopic techniques (UV/Vis, CD, NMR, EPR) to probe its behavior in solution. Studies on the binding properties of the complex performed with the azide anion as a probe showed that the ligand preferably binds to the Cu_A centers of the complex and only weakly to the Cu_B center. The EPR spectra showed the existence of a strong coupling between one of the two Cu_A centers and the Cu_B center, which appears to be mediated by a hydroxido-bridging ligand. Further information about metal binding was obtained by analyzing the NMR spectra of the trinuclear Zn^{II}_3–PHI complex, which serves as an analogue of the extremely oxygen sensitive Cu^I_3–PHI complex. The latter complex does not form a stable dioxygen adduct at low temperature, but exhibits an interesting monooxygenase activity. This was studied at low temperature using p-chlorophenolate as a substrate; the formation of 4-chlorocatechol in sizeable yield indicates that some of the very reactive Cu_nO_2 intermediate should be involved.

(© Wiley-VCH Verlag GmbH & Co. KGaA, 69451 Weinheim, Germany, 2008)

Introduction

Research on low-molecular weight biomimetic metal complexes is a widely used approach by inorganic chemists to simulate the main spectroscopic, structural, and reactivity features of large biological macromolecules containing metal ions. To this end, bioinorganic chemists typically synthesized and studied model complexes designed to reproduce key structural features of the metal centers in the biopolymers.[1] The model approach has provided many valuable insights into structural and mechanistic metallobiochemistry, including the metal oxidation states, the effects of distance and medium on electron-transfer rates, the role of steric and electronic factors in controlling ligand binding, and the identification of the intermediates that play an important role in a variety of enzyme-catalyzed reactions. Biomimetic copper complexes, in particular, have been very widely studied as models for copper enzymes with oxidase or oxygenase activity,[2] also because their activity bears great promise for the development of new and efficient catalysts for oxidation reactions.[3] Dinuclear complexes have mostly been employed in these studies, while the potentially larger family of trinuclear complexes is still little developed, although it has been known for a while that the arrangement of three copper ions bound to a total of eight histidine ligands is the key structural feature of the active site of multicopper blue oxidases, as a formal assembly of type 2–type 3 copper centers.[4] Recently, we developed a family of polydentate ligands carrying eight nitrogen donors and containing either a central didentate diamine or amino acid residue,[5] acting as a chiral spacer between two chelating arms having tridentate donors, or an achiral piperazine residue connected with two chiral tridentate arms derived from histidine residues.[6] The corresponding trinuclear copper(II) complexes represent a new family of potential structural and functional models for the multinuclear sites of copper enzymes. Besides serving as biomimetic models for the metalloprotein active sites, such polynuclear complexes could be exploited as new catalytic systems for synthetic transformations, e.g. oxidations, of potential applicative interest. Our previous studies of stereoselective

[a] Dipartimento di Chimica Inorganica, Metallorganica e Analitica, Università di Milano, Istituto ISTM-CNR,
   Via Venezian 21, 20133 Milano, Italy
[b] Dipartimento di Chimica Organica e Industriale, Università di Milano,
    Via Venezian 21, 20133 Milano, Italy
[c] Dipartimento di Chimica Generale, Università di Pavia,
    Via Taramelli 12, 27100 Pavia, Italy
    Fax: +39-0382-528544
    E-mail: bioinorg@unipv.it
[d] Department of Molecular Biosciences, University of Oslo,
    0316 Oslo, Norway
🖳 Supporting information for this article is available on the WWW under http://www.eurjic.org or from the author.

oxidations with chiral trinuclear complexes[5c,5d,7] show that compounds of this type are indeed promising, because depending on the ligand design they can be programmed to use one of the metal centers or a ligand fragment as the site of chiral discrimination of the substrate.[2d] However, the increased structural complexity of trinuclear complexes with respect to e.g. their dinuclear counterparts makes it more difficult to make predictions on important aspects of their reactivity, such as the degree of communication between the metal centers or the mode of substrate interaction with the complex. Azide proved to be a useful small ligand probe in a recent investigation of the accessibility and the possible mode of binding at the copper(II) centers of the trinuclear complex derived from a binaphthyl-2,2′-diamine,[5c] since the copper(II)–azido interaction can be characterized by a variety of spectroscopic techniques. This approach is followed here to study the ligand binding behavior of the trinuclear copper(II) complex derived from the ligand PHI (Scheme 1).[6] In addition, we also report the monooxygenase activity exhibited by the reduced form of the complex on p-chlorophenolate at low temperature.
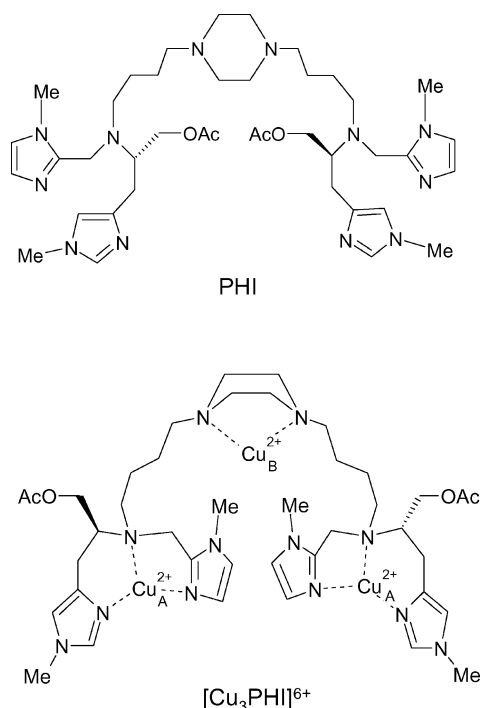
Scheme 1. Structure of the ligand PHI and its trinuclear complex [Cu₃PHI]⁶⁺.

Results and Discussion

Characterization of the Azido Adducts of Copper–PHI Complexes

For the interpretation of the azido-binding properties of the trinuclear complex [Cu₃PHI]⁶⁺, it is useful to compare its behavior with that of the expectedly simpler dinuclear counterpart of this complex, [Cu₂PHI]⁴⁺. Various azido ad-

ducts of both the dinuclear and trinuclear complexes were indeed easily obtained, because of their apparent high affinity for small anionic ligands. The electronic and CD spectra of the isolated azido adducts are shown in Figure 1 and Figure 2 for [Cu₂PHI]⁴⁺ and [Cu₃PHI]⁶⁺, respectively. The near-UV region of the electronic spectra of all the copper(II)–PHI complexes shows a well defined, but somewhat asymmetric band of moderate intensity, with a maximum in the range 270–290 nm and a tail extending up to about 350 nm. As already reported,[6] the origin of this band must be that of a charge-transfer type within the copper(II)–imidazole and copper(II)–amine chromophores. At lower energy, the spectra of the azido adducts exhibit the characteristic absorption band due to the $\pi(N_3^-) \rightarrow Cu^{II}$ LMCT, with a maximum near 400 nm, and the broad envelope of the LF transitions, with a maximum near 650 nm and a prominent shoulder above 700 nm. In the CD spectra, both types of electronic bands show multicomponent structures from an evident exciton couplet[8] for the azido–Cu^{II} LMCT and a better resolution of the d–d transitions within the LF band. The symmetric shape of the LMCT optical bands indicates that azide binds in the terminal mode to the copper(II) centers in all cases,[9] while bridging azide gives rise to characteristic multicomponent LMCT bands.[10,11] The sizeable intensity of the azido–Cu^{II} LMCT band indicates that it is electric dipole allowed; this implies that there must be good overlap between the donor, $\pi(N_3^-)$, and acceptor, $d_{x^2-y^2}$, orbitals,[11] and therefore that azide binds in the Cu equatorial plane. In addition, as observed
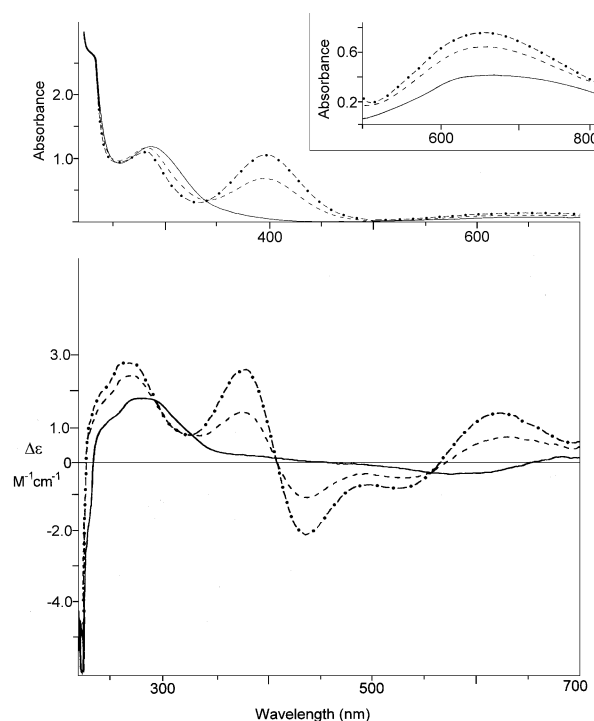

Figure 1. Electronic and circular dichroism spectra of [Cu₂PHI]⁴⁺ (——), [Cu₂PHI(N₃)]³⁺ (- - -), and [Cu₂PHI(N₃)₂]²⁺ (– · – ·) in MeOH/MeCN, 9:1 (v:v) solution. The inset shows the expanded region of the d–d transitions.

systematically for copper(II)–azido complexes,[9,10–12] azide binding is accompanied by an increase in the absorption of the LF bands.
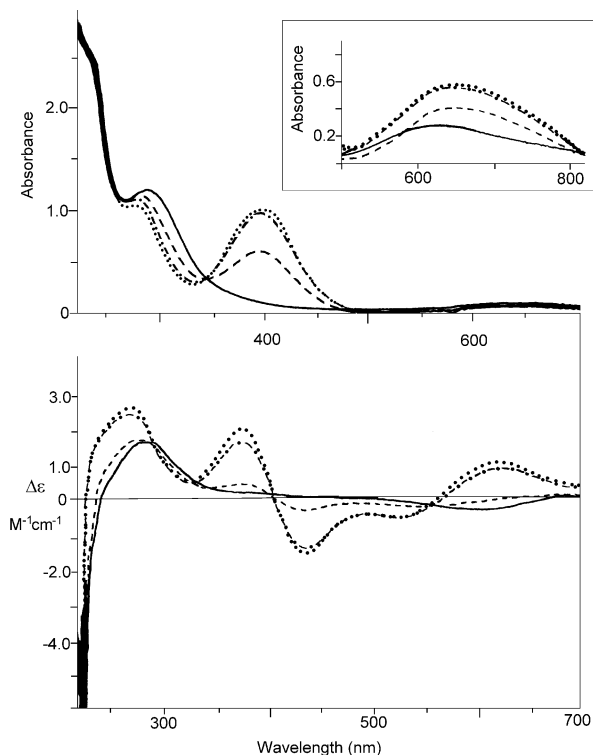

Figure 2. Electronic and circular dichroism spectra of $[Cu_3PHI]^{6+}$ (——), $[Cu_3PHI(N_3)]^{5+}$ (- - -), $[Cu_3PHI(N_3)_2]^{4+}$ (– · – ·), and $[Cu_3PHI(N_3)_3]^{3+}$ (· · ·) in MeOH/MeCN, 9:1 (v:v) solution. The inset shows the expanded region of the d–d transitions.
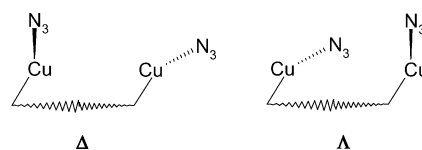
For the azido adducts of $[Cu_2PHI]^{4+}$ the interpretation of the CD spectra is relatively simple. Here we have two identical copper(II) centers bound to A sites[6] where azide molecules can bind. The observation of a CD exciton couplet within the azido–Cu[II] LMCT band can only be explained by the simultaneous presence of two bound azide molecules, one per each copper(II) center, as the mechanism generating the exciton is coupling between the transition moments of the two electric dipole LMCTs. The exciton couplet is also clearly observable in the CD spectrum of $[Cu_2PHI(N_3)]^{3+}$, indicating that in solution some redistribution of azide molecules occurs, but the CD intensity is clearly maximized for the bis adduct $[Cu_2PHI(N_3)_2]^{2+}$. In contrast, the absence of magnetic dipole character for the LMCT implies negligible optical activity for the bound azido molecule in the complex $[Cu_2PHI(N_3)]^{3+}$, in line with previous results using mononuclear copper(II) complexes with chiral tridentate ligands.[9] In the d–d region, the intensity of the CD bands is much stronger for the azido adduct $[Cu_2PHI(N_3)_2]^{2+}$ with respect to the precursor complex $[Cu_2PHI]^{4+}$ but, more importantly, the dominant Cotton effects are reversed (Figure 1). This indicates that azide binding reduces the conformational mobility of the ligand and causes a change from the slight preference for the λ conformation of the histidine chelate ring in $[Cu_2PHI]^{4+}$,[6]

to the strong preference for the δ conformation in $[Cu_2-PHI(N_3)_2]^{2+}$. In the latter conformation all four nitrogen donor ligands occupy the equatorial coordination positions in the plane of the copper(II) ions of the presumably square-pyramidal structure, as shown in Scheme 2. The equatorial coordination of azide is confirmed by the EPR spectroscopic data (see below) and is in line with the azide-binding behavior of mononuclear copper(II) complexes with a similar (neutral charge) tridentate N_3-donor environment.[9]
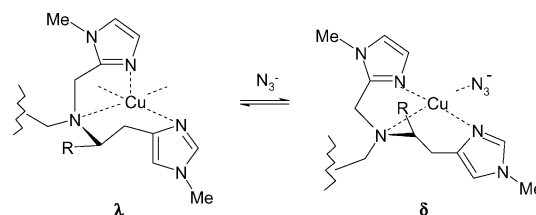
Scheme 2. Conformational effect associated with the azido binding equilibria at the Cu_A sites (R = CH_2OAc).

From the CD sign pattern of the exciton couplet it is possible to make a proposal on the relative orientation of the two copper(II)–azido chromophores in $[Cu_2PHI-(N_3)_2]^{2+}$, as the exciton couplet can only be generated by a skew arrangement of the transition dipole moments associated with the two LMCT transitions. Since azide binds in the Cu equatorial plane and the donor, $\pi(N_3^-)$, and acceptor, $d_{x^2-y^2}$, orbitals are coplanar, we can assume that the direction of the LMCT transition moment is roughly parallel to the Cu–N bond for each of the two copper(II)–azido chromophores. Therefore, the negative CD component at lower energy of the exciton couplet indicates the two Cu[II]–azido moieties in $[Cu_2PHI(N_3)_2]^{2+}$ must be arranged according to a Δ configuration[13] between the skewed Cu–N axial bonds, as shown schematically in the following structure.

For the azido adducts of $[Cu_3PHI]^{6+}$ the interpretation of the CD spectra is more complicated, because there are more possibilities for the ligand to bind to the metal centers, and a complete picture needs support from the EPR spectroscopic experiments. The binding of the first azide molecule yields complex $[Cu_3PHI(N_3)]^{5+}$, which exhibits a rather intense LMCT band in the electronic spectrum, but negligible optical activity (Figure 2). This could be interpreted both in terms of binding of the anion to one Cu_A or, preferably, to the Cu_B center, which is only bound through the didentate piperazine residue to PHI (Scheme 1). However, the EPR data clearly show that this adduct is of type Cu_A–N_3^-, since Cu_B is strongly coupled to the other Cu_A center through a hydroxo ligand and may actually not be easily accessible. The intensity of the LMCT band and the EPR spectrum of this adduct show that azide binds in an equato-

rial coordination position, reproducing the situation shown in Scheme 2. Ligation of the second azide molecule to $[Cu_3PHI]^{6+}$ yields the bis adduct $[Cu_3PHI(N_3)_2]^{4+}$, which is characterized by the appearance of an exciton couplet in the CD spectrum similar to that exhibited by $[Cu_2PHI(N_3)_2]^{2+}$. Here the two chromophores involved in the coupling must be identical and therefore we conclude that both azide ligands are mostly bound to Cu_A sites. Actually, the somewhat lower intensity of the CD exciton doublet for $[Cu_3PHI(N_3)_2]^{4+}$ than for $[Cu_2PHI(N_3)_2]^{2+}$ is contrary to expectation, as the two copper(II)–azido chromophores should be closer in space in the trinuclear complex, and indicates that the orientation of the coupled azido–Cu^{II} LMCTs is slightly different, with a smaller dihedral angle between the coupled transition moments, or even that a minor fraction of azide may be bound to Cu_B. Binding of the third azide molecule in $[Cu_3PHI(N_3)_3]^{3+}$ produces small hyperchromic effects on the near-UV optical and CD LMCT bands, but a small shift to lower energy of the absorption λ_{max} suggests the involvement of Cu_B at this stage. The small increase in the intensity of the LMCT band is consistent with the binding of N_3^- to Cu_B in an axial coordination position, since in this case the donor and acceptor orbitals are orthogonal.[9]

Ligand Binding Experiments

The complex $[Cu_2PHI]^{4+}$ binds azide molecules with rather high affinity and it is interesting to note that only two azide ligands are bound to the complex, because even at very high concentrations of the azide anion the near-UV LMCT band has the same intensity as that obtained after the addition of 2 equiv. of the ligand. The two binding steps can be separated and the binding constants can be estimated by spectrophotometric titration, since the two steps are characterized by different isosbestic points (at 340 nm in the first and 348 nm in the second step). The Hill equation was used for the determination of the equilibrium constants of the adducts, yielding the equilibrium constants K_1 = 18000 M^{-1} and K_2 = 16400 M^{-1} for the two steps. Azide binding experiments were also performed with the trinuclear complex $[Cu_3PHI]^{6+}$ and in this case three azide molecules are apparently bound with very high affinity, as shown by the stoichiometry of the adducts isolated in the solid state and from the solution CD studies. However, even though the shape of the LMCT band changes slightly upon successive additions of azide, in this case it has been impossible to separate the process into three binding steps.

EPR Experiments and Analysis

The EPR spectra of the complexes $[Cu_2PHI]^{4+}$ and $[Cu_3PHI]^{6+}$ and their azido adducts were recorded in diluted glassy solutions and their observed traces are depicted in Figures 3 and 4, respectively. The relevant spin-Hamilto-

nian parameters are collected in Table 1 together with the calculated spin concentrations for both complexes and adducts. A comparison of the EPR traces of the starting dinuclear and trinuclear copper(II) complexes (see parts a in Figures 3 and 4) shows that these complexes have an almost identical pattern, with spin-Hamiltonian parameters consistent with the metal bound at the A site in a distorted square-pyramidal fashion. This observation contrasts with the fact that in $[Cu_3PHI]^{6+}$ two different chelating sites for the Cu^{II} ions are present, and therefore an overlap of signals for the metals bound to the A and B sites should be observed. This is shown in Figure 1S (see Supporting Information), where the simulated EPR spectra for Cu^{II} ions coordinated at the A and B sites are depicted. However, in the dinuclear complex, the spin concentration accounts for two noninteracting $S = 1/2$ systems while for the trinuclear complex only one Cu^{II} ion associated with the A site can be observed. No changes in the EPR spectroscopic envelope arising from either a triplet species or different "types" of copper ions could be observed for the trinuclear complex upon increasing or decreasing the microwave power, or upon increasing (up to 150 K) or decreasing (down to 77 K) the sample temperature. These results indicate that a rather strong antiferromagnetic interaction ($|2J| > -160$ cm^{-1}) occurs between one copper at the A site and Cu_B and this interaction needs to be mediated by a bridging group, Cu_A–X–Cu_B, (vide infra) rather than act through a dipolar through-space interaction. Even more unexpected is the binding behavior of the small ligand probe azide molecule
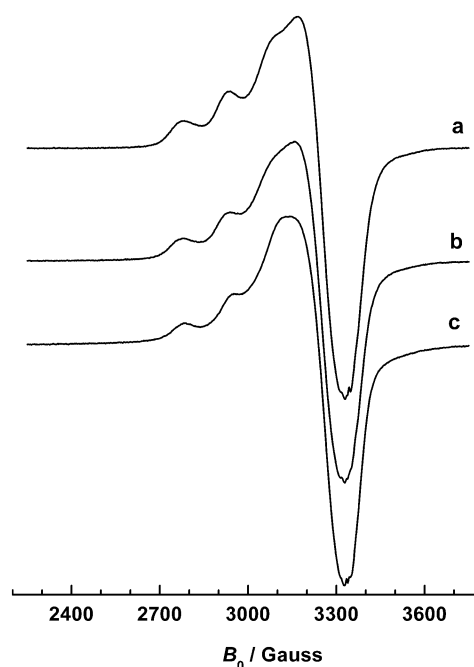

Figure 3. EPR spectra of $[Cu_2PHI]^{4+}$ (3.2 mM in MeCN/MeOH, 8:2, v/v) and its azido adducts: (a) $[Cu_2PHI]^{4+}$, (b) $[Cu_2PHI]^{4+}$ + 1 equiv. N_3^-, (c) $[Cu_2PHI]^{4+}$ + 2 equiv. N_3^-. Instrumental parameters: frequency (a) 9.415731 GHz, (b) 9.415271 GHz, (c) 9.415276 GHz, then 100 kHz modulation frequency, 5.0 gauss modulation amplitude, 1.0 mW microwave power, 84 s sweep time, 82 ms time constant, 5 scans, $T = 100$ K.

to $[Cu_2PHI]^{4+}$ and $[Cu_3PHI]^{6+}$. As shown in parts b of Figures 3 and 4, no clear differentiation between the dinuclear and trinuclear complexes, respectively, can be observed in the EPR patterns, apart from the increased strength of the Cu^{II} tetragonal field upon azide binding, signalled by a decrease in $g_{\parallel}$ values and an increase in $A_{\parallel}$ values (Table 1), with spectral features always associated with a Cu^{II} ion bound to the A site.

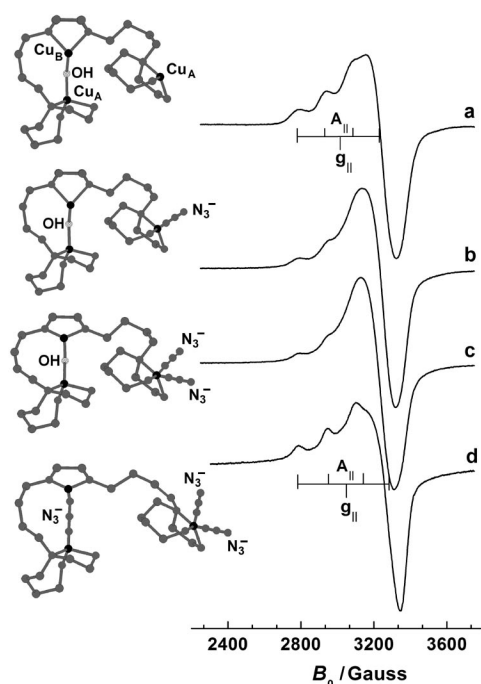Figure 4. EPR spectra of $[Cu_3PHI]^{6+}$ (6.3 mM in MeCN/MeOH, 8:2, v/v) and its azido adducts: (a) $[Cu_3PHI]^{6+}$, (b) $[Cu_3PHI]^{6+}$ + 1 equiv. N_3^-, (c) $[Cu_3PHI]^{6+}$ + 2 equiv. N_3^-, (d) $[Cu_3PHI]^{6+}$ + 3 equiv. N_3^-. Instrumental parameters: frequency (a) 9.416016 GHz, (b) 9.416020 GHz, (c) 9.415563 GHz, (d) 9.41596 GHz, then 100 kHz modulation frequency, 5.0 gauss modulation amplitude, 1.6 mW microwave power, 84 s sweep time, 82 ms time constant, 5 scans, T = 100 K.

Table 1. Spin-Hamiltonian parameters for the copper–PHI complexes and their azido adducts.

Ligand	$G_{\parallel}$	$A_{\parallel}$ ($\times 10^{-4}$ cm^{-1})	$g_{\perp}$	Spin[a]
$[Cu_2PHI]^{4+}$	2.231	167	2.071	2.0 ± 0.2
$[Cu_2PHI(N_3)]^{3+}$	2.224	169	2.075	1.9 ± 0.2
$[Cu_2PHI(N_3)_2]^{2+}$	2.219	172	2.080	2.0 ± 0.1
$[Cu_3PHI]^{6+}$	2.232	166	2.070	1.1 ± 0.1
$[Cu_3PHI(N_3)]^{5+}$	2.211	173	2.084	1.2 ± 0.2
$[Cu_3PHI(N_3)_2]^{4+}$	2.210	174	2.087	1.2 ± 0.2
$[Cu_3PHI(N_3)_3]^{3+}$	2.208	178	2.094	0.9 ± 0.1
$[Cu_3PHI]^{6+}$	(Cu$_A$) 2.234	163	–	–
(pH = 5)	(Cu$_B$) 2.208	183	ca. 2.07	1.5 ± 0.2

[a] A standard solution of 1 mM CuEDTA in MeOH/MeCN, 2:8 (v/v), was employed to evaluate the sample spin concentration.

While in the case of $[Cu_2PHI]^{4+}$ these results are consistent with terminal binding of the N_3^- ion to the two isolated and identical copper ions, for $[Cu_3PHI]^{6+}$ different spin-

Hamiltonian parameters associated with multiple species would be expected upon replacement or destabilization of the bridging group between the Cu$_A$ and Cu$_B$ centers when these sites interact with azido molecules. Because the sample spin concentration always accounts for one isolated S = 1/2 system we suggest that the first two azide ligands have a higher affinity for the Cu^{II} ion at the unbridged A site. Eventually, a further N_3^- molecule binding to the coupled Cu$_A$–X–Cu$_B$ center replaces the previous bridging group. Furthermore, a similar size for the Cu$_A$–Cu$_B$ antiferromagnetic interaction as that previously estimated should also hold here (Figure 4, d). In order to investigate the low accessibility of the coupled Cu$_A$–X–Cu$_B$ site, the EPR features of $[Cu_3PHI]^{6+}$ were studied as a function of pH and the results are presented in Figure 5. Upon decreasing the pH down to 5, two different types of copper signals appear in the spectrum, with Cu$_B$ exhibiting rather strong tetragonal distortion as expected. This pH effect is therefore linked with the displacement of a strongly bridged Lewis base, which can be associated with a hydroxido/water molecule. However, since the spin concentration accounted for only 1.5 Cu^{II} ions and no Δm_s = 2 transition is observed, we propose that the equilibrium between bridged and unbridged Cu$_A$···Cu$_B$ centers leads to a conformational interconversion between a folded (bridged) and an open (unbridged) structure of the complex, where the copper ions are noninteracting and therefore well separated in space. Unfortunately, upon further decreasing the pH of the medium, the ligand undergoes partial protonation, with release of a significant portion of Cu^{II} ions associated with the B site, thus hindering an unambiguous estimation of the pK_a of the bridging X group.
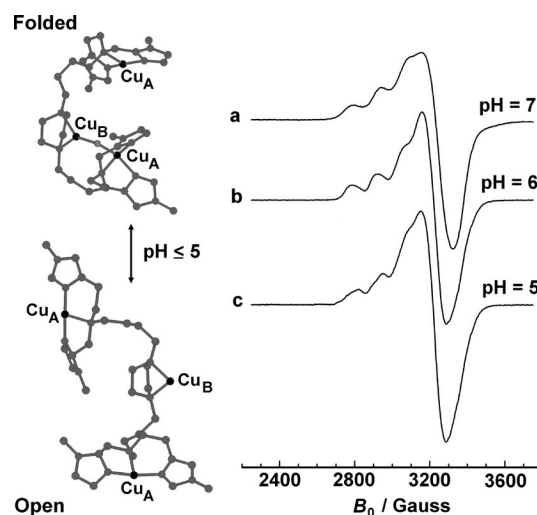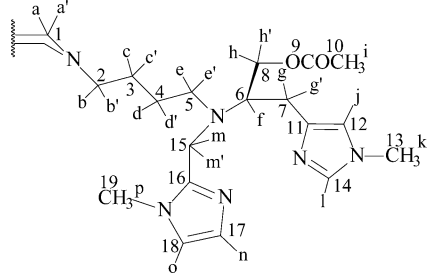

Figure 5. EPR spectra of $[Cu_3PHI]^{6+}$ (3.8 mM in MeOH/aqueous phosphate buffer 30:1, v/v) as a function of pH. Instrumental parameters: frequency (a) 9.416033 GHz, (b) 9.416042 GHz, (c) 9.415988 GHz, then 100 kHz modulation frequency, 5.0 gauss modulation amplitude, 1.6 mW microwave power, 84 s sweep time, 82 ms time constant, 10 scans, T = 90 K.

NMR Experiments

Given the extreme oxygen sensitivity of the copper(I) complex [Cu₃PHI]³⁺, we thought it useful to investigate the zinc(II) analogue of this complex by NMR spectroscopic experiments in order to gain information about the sites of metal binding, since the structural preferences of the two d^{10} metal ions should be similar. The comparative NMR spectroscopic experiments between PHI and the zinc(II) complex were carried out in [D₆]acetone because both compounds are sufficiently soluble in it, and the best peak resolution was obtained. The assignment of the ¹H and ¹³C NMR signals in the spectrum of PHI, Table 2, was based on the expected chemical shifts and *J*-coupling patterns, and was confirmed by two-dimensional NMR spectroscopic experiments (Figure 2S). The assignment of aromatic resonances was easily done from a combination of ¹H-¹H COSY, DEPT135, and ¹H-¹³C HSQC spectra. An unambiguous assignment of aliphatic resonances was more difficult and could be obtained from the combination of ¹H-¹H COSY, ¹H-¹H TOCSY, DEPT135, ¹H-¹³C HSQC, and ¹H-¹³C HMBC spectra. With a ¹H-¹³C HSQC experiment all the direct connections between H and C atoms could be detected. A comparison of ¹³C and DEPT135 spectra gave the positions of the methyl carbons 10, 13, and 19; then, long-range heteronuclear correlation with them allowed the assignment of the quaternary carbons 9, 11, and 16. The attribution of C-6 and proton f resonances was possible with DEPT 135 and HSQC; with COSY, TOCSY, HSQC,

Table 2. ¹H and ¹³C NMR chemical shift (δ, ppm) assignments for the ligand PHI in [D₆]acetone solution.

¹H	δ	¹H	δ	¹H	Δ [ppm]
A	2.30	e	2.59	J	6.78
a′	2.30	e′	2.59	K	3.67
b	2.19	f	3.34	L	7.36
b′	2.19	g	2.52	M	3.84
c	1.38	g′	2.81	m′	3.90
c′	1.38	h	4.09	N	6.76
d	1.32	h′	4.18	O	6.97
d′	1.32	i	1.86	P	3.69
¹³C	δ	¹³C	δ	¹³C	Δ [ppm]
1	54.5	7	27.6	13	33.6
2	59.4	8	65.1	14	138.6
3	25.6	9	171.6	15	49.7
4	27.7	10	21.5	16	147.3
5	51.2	11	141.6	17	127.8
6	61.0	12	118.8	18	123.1
				19	33.9

Table 3. ¹H and ¹³C NMR chemical shift (δ, ppm) assignments for the [Zn₃PHI]⁶⁺ complex in [D₆]acetone solution.[a]
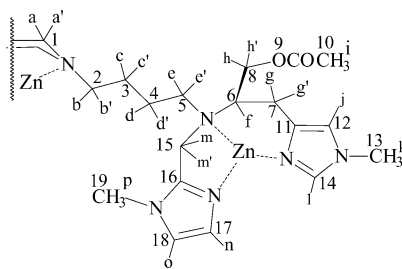
¹H	δ	Δ ($\delta_c - \delta_l$)	¹H	δ	Δ ($\delta_c - \delta_l$)	¹H	δ	Δ ($\delta_c - \delta_l$)
a	3.25	+0.95	e	3.14	+0.55	j	7.28	+0.50
a′	3.25	+0.95	e′	3.14	+0.55	k	3.88	+0.21
b	3.54	+1.35	f	4.28	+0.94	l	8.18	+0.82
b′	3.54	+1.35	g	3.07	+0.55	m	4.67	+0.83
c	1.79	+0.41	g′	3.07	+0.26	m′	4.67	+0.77
c′	1.79	+0.41	h	4.30	+0.21	n	7.23	+0.47
d	1.68	+0.36	h′	4.46	+0.28	o	7.42	+0.45
d′	1.68	+0.36	i	2.16	+0.30	p	3.84	+0.15
¹³C	δ	Δ ($\delta_c - \delta_l$)	¹³C	δ	Δ ($\delta_c - \delta_l$)	¹³C	δ	Δ ($\delta_c - \delta_l$)
1	58.4	+3.9	7	27.0	+0.6	13	35.6	+2.0
2	61.6	+2.2	8	65.1	0.0	14	141.5	+2.9
3	23.4	−2.2	9	171.6	0.0	15	47.0	−2.7
4	24.2	−3.5	10	21.5	0.0	16	149.9	+2.6
5	57.7	+6.5	11	139.4	−2.2	17	126.1	−1.7
6	62.6	+1.6	12	121.2	+2.4	18	125.8	+2.7
						19	34.2	+0.3

[a] Δ ($\delta_c - \delta_l$) = $\delta_{complex} - \delta_{ligand}$.

and HMBC, this allowed the assignment of the resonances of methylene protons g, g′, h, h′, m, and m′ and carbons 7, 8, and 15. The lack of correlations in the COSY and TOCSY spectra allowed the identification of protons a and a′ and carbon 1; then, HMBC let us unambiguously assign protons b, b′, e, and e′ and carbons 2 and 5. Finally COSY and TOCSY experiments gave the assignment of protons c, c′, d, and d′ and carbons 3 and 4.

The corresponding NMR spectroscopic data for the complex $[Zn_3PHI]^{6+}$ are given in Table 3. The assignment of the ^1H and ^{13}C NMR signals was basically performed by two-dimensional NMR experiments (Figure 3S). Assignment of aromatic resonances was easily done by a combination of ^1H-^1H COSY, DEPT135, and ^1H-^{13}C HSQC experiments. The presence of zinc(II) ions induced a downfield shift of many signals in the aliphatic region of the spectra, thus the unambiguous assignment of resonances in this area was very difficult and could be obtained from the combination of all the techniques already used for PHI. Methyl protons i, k, and p and the corresponding carbons 10, 13, and 19 were assigned from DEPT135, ^{13}C and ^1H-^{13}C HSQC spectra; a comparison between the DEPT135 and ^{13}C NMR signals, combined with the ^1H-^{13}C HMBC spectrum, also gave the positions of the quaternary carbons **9**, 11, and 16. Protons c, c′, d, and d′ (and consequently carbons 3 and 4) are less affected by zinc(II) coordination than the other aliphatic nuclei and were simply assigned by COSY and TOCSY spectra. Finally, assignment of the signals of protons a, a′, b, b′, e, e′, f, g, g′, h, h′, m, and m′, and the corresponding carbons 1, 2, 5, 6, 7, 8, and 15 was only possible by a combination of COSY, TOCSY, HSQC, and HMBC spectra. Although, in general, all proton resonances are downfield shifted in the spectrum of the Zn^{II}_3PHI complex, because of the high positive charge, large downfield shifts of more than +0.5 ppm are observed for the groups adjacent to the eight nitrogen donor atoms (Table 3). Similar observations can be made for the shifts in the carbon NMR spectra, where the size of the shift is often of several ppm. This is consistent with the suggested coordination structure of the complex, with the three Zn^{II} ions bound at the same A and B sites as the Cu^{II} analogue (Scheme 1). We can therefore presume that a similar arrangement is adopted in the corresponding $[Cu^I_3PHI]^{3+}$ complex.

Phenol Monooxygenase Activity of the $[Cu^I_3PHI]^{3+}$ Complex

While there are now several dinuclear copper complexes that are able to reproduce the biomimetic phenol hydroxylation performed by tyrosinase,[2,14] the potential activity of trinuclear copper complexes in a similar reaction has never been reported. In these preliminary experiments we thus wanted to assess whether $[Cu^I_3PHI]^{3+}$ was active in the phenol hydroxylation and, possibly, to characterize a Cu_nO_2 adduct of this complex at low temperature. The addition of dry O_2 to a solution of $[Cu^I_3PHI]^{3+}$ in CH_2Cl_2 or acetone at –78 °C did not produce appreciable spectral changes, in-

dicating that Cu_nO_2 adducts of this complex are not sufficiently stable to be observed under these conditions. Probably, unlike the corresponding trinuclear copper(II) complex, which spontaneously forms a hydroxo bridge in solution that keeps two of the three ions in close proximity, here the three copper(I) ions are kept far from each other in solution, and too large conformational changes are necessary to allow a dioxygen moiety to connect two or all three metal ions in a stable complex.

When a cooled solution of sodium p-chlorophenolate in CH_2Cl_2 was added to the oxygenated $[Cu^I_3PHI]^{3+}$ solution in CH_2Cl_2 at low temperature a significant amount of 4-chlorocatechol was formed, as shown by HPLC analysis and NMR spectra performed on the organic extracts after workup of the reaction mixture. The yields of 4-chlorocatechol were 10% and 65% with respect to the initial Cu^I complex when 1.0 and 10.0 equiv. of p-chlorophenolate, respectively, were used in the reaction. The catechol was the only organic reaction product, and neither the corresponding o-quinone derivative nor C–C or C–O phenol coupling dimers were formed. Thus, in spite of the lack of a build-up of any Cu_nO_2 adduct, the formation of sizeable amounts of 4-chlorocatechol strongly suggests that some type of Cu_nO_2 species forms in a pre-equilibrium upon treatment of the copper(I) complex with O_2. A low value of the equilibrium constant for the formation of the Cu_nO_2 adduct prevents the accumulation of this species to a detectable extent at the temperature of the experiments.[2] Upon reaction with p-chlorophenolate in the presence of dioxygen, the copper(I) complex is directly converted into the corresponding copper(II) complex. As a consequence we cannot determine the nature of the active species because both the possible structures for dinuclear adducts, $(\mu$-η^2:η^2-peroxido)dicopper(II) and bis(μ-oxido)dicopper(III), or eventually any new Cu_3O_2 species, are active in the phenol hydroxylation reaction. We are currently developing new ligands related to PHI but containing bulkier substituents with the aim of favoring a more closed conformation of the ligand in the tris-copper(I) complex and thereby stabilizing a dioxygen adduct at low temperature.

Experimental Section

Materials and Physical Methods: All reagents were of the highest grade commercially available and were used as received. Optical spectra were recorded with HP 8452A or 8453 diode array spectrophotometers. Circular dichroism (CD) spectra were obtained with a Jasco J-500 dichrograph using quartz cells with a 0.1–1 cm path length. NMR spectra were recorded with Bruker AVANCE 400 or Bruker AVANCE 500 spectrometers operating at 9.37 and 11.71 T, respectively. EPR spectra were recorded in a degassed solution using a Bruker X-band spectrometer ESP300 E, equipped with an NMR gaussmeter (Bruker ER035), a frequency counter (Bruker ER 041 XK), and a variable-temperature control continuous-flow N_2 cryostat (Bruker B-VT 2000). The software programs WINEPR (v. 2.11) and SimFonia (v. 1.25) were provided by Bruker. Integration of the EPR signals was performed using a 1 mM copper(II)-EDTA solution under the same conditions, while a DPPH free radical ($g = 2.0036$) was used as the reference for the g value correc-

tions. The azido adducts that were studied by EPR spectroscopy were prepared by overnight incubation at 4 °C of solutions of the copper complexes with the calculated amount of azide in a closed reaction vessel under anaerobic conditions. The low-temperature experiments were performed with a custom designed immersible fiber-optic quartz probe (HELLMA) fitted to a Schlenk vessel and connected with the diode array spectrophotometer HP 8453. The analysis of the reaction mixtures derived from oxygenation of *p*-chlorophenol was performed by HPLC using a Jasco MD-1510 instrument with diode array detection.

Caution! Although the perchlorate salts reported here seem to be stable to shock and heat they should be handled with great care. Azido complexes are also potentially explosive. No problems were encountered while studying small amounts of the adducts.

Synthesis of the Ligand and Copper(II) Complexes: The multistep synthesis of the ligand piperazine-1,4-bis(4-{*N*-[1-acetoxy-3-(1-methyl-1*H*-imidazol-4-yl)]-2-propyl}-*N*-(1-methyl-1*H*-imidazol-2-ylmethyl)aminobutyl) (PHI), and the corresponding complexes, [Cu$_2$PHI][ClO$_4$]$_4$ and [Cu$_3$PHI][ClO$_4$]$_6$, was reported previously.[6]

Synthesis of the Azido Complexes: The general synthesis of the azido complexes, derived from both [Cu$_2$PHI][ClO$_4$]$_4$, and [Cu$_3$-PHI][ClO$_4$]$_6$, was carried out at room temp. by mixing methanolic solutions of the complexes (ca. 0.1 mmol) and the appropriate amount of sodium azide in methanol in order to obtain the adduct of desired stoichiometry. The resulting blue-green or dark green solutions were concentrated to a small volume and allowed to stand in a refrigerator until precipitation of the product occurred. The precipitate thus formed was filtered off, washed with a small amount of methanol, and dried under vacuum. When no spontaneous precipitation took place, even after prolonged cooling of the solution, the precipitation of the adduct was induced by the addition of a small amount of diethyl ether to the cold solutions. The products were then filtered off, washed with small amounts of cold water and diethyl ether, and dried under vacuum over CaCl$_2$.

[Cu$_2$PHI(N$_3$)][ClO$_4$]$_3$·4H$_2$O: Yield 75%. C$_{40}$H$_{64}$Cl$_3$Cu$_2$N$_{15}$O$_{16}$· 4H$_2$O (1316.55): calcd. C 36.40, H 5.51, N 15.96; found C 36.44, H 5.61, N 16.07. UV/Vis (MeOH/MeCN, 9:1 v:v): λ_{max} (ε) = 226 sh (17800), 282 (4900), 396 (3500), 638 nm (470 M^{-1} cm^{-1}). CD (MeOH/MeCN, 9:1 v:v): λ_{max} ($\Delta\varepsilon$) = 245 sh (+1.50), 278 (+2.37), 377 (+1.41), 435 (–0.96), 495 (–0.30), 535 (–0.40), 635 nm (+ 0.67 M^{-1} cm^{-1}).

[Cu$_2$PHI(N$_3$)$_2$][ClO$_4$]$_2$·2H$_2$O: Yield 70%. C$_{40}$H$_{64}$Cl$_2$Cu$_2$N$_{18}$O$_{12}$· 2H$_2$O (1223.10): calcd. C 39.28, H 5.60, N 20.62; found C 39.11, H 5.76, N 20.90. UV/Vis (MeOH/MeCN, 9:1 v:v): λ_{max} (ε) = 226 sh (19600), 278 (4700), 396 (4450), 642 nm (518 M^{-1} cm^{-1}). CD (MeOH/MeCN, 9:1 v:v): λ_{max} ($\Delta\varepsilon$) = 250 sh (+ 2.10) 275 (+2.80), 380 (+2.75), 440 (–2.00), 495 (–0.60), 535 (–0.67), 630 nm (+1.42 M^{-1} cm^{-1}).

[Cu$_3$PHI(N$_3$)][ClO$_4$]$_5$·5H$_2$O: Yield 80%. C$_{40}$H$_{64}$Cl$_5$Cu$_3$N$_{15}$O$_{24}$· 5H$_2$O (1597.01): calcd. C 30.08, H 4.67, N 13.16; found C 30.44, H 4.71, N 13.22. UV/Vis (MeOH/MeCN, 9:1 v:v): λ_{max} (ε) = 228 sh (20400), 282 (4860), 396 (2660), 640 nm (380 M^{-1} cm^{-1}). CD (MeOH/MeCN, 9:1 v:v): λ_{max} ($\Delta\varepsilon$) = 252 sh (+0.93), 283(+ 1.70), 380 (+0.45), 438 (–0.33), 488 (–0.19), 553 nm (–0.30 M^{-1} cm^{-1}).

[Cu$_3$PHI(N$_3$)$_2$][ClO$_4$]$_4$·3H$_2$O: Yield 68%. C$_{41}$H$_{68}$Cl$_4$Cu$_3$N$_{18}$O$_{21}$· 3H$_2$O (1503.56): calcd. C 31.95, H 4.69, N 16.77; found C 31.41, H 4.77, N 16.89. UV/Vis (MeOH/MeCN, 9:1 v:v): λ_{max} (ε) = 228 sh (21500), 278 (4800), 396 (4350), 642 nm (520 M^{-1} cm^{-1}). CD (MeOH/MeCN, 9:1 v:v): λ_{max} ($\Delta\varepsilon$) = 250 sh (+2.02), 276 (–2.57), 380 (+1.59), 438 (–1.52), 498 (–0.46), 525 (–0.57), 622 nm (+0.85 M^{-1} cm^{-1}).

[Cu$_3$PHI(N$_3$)$_3$][ClO$_4$]$_3$: Yield 65%. C$_{40}$H$_{64}$Cl$_3$Cu$_3$N$_{21}$O$_{16}$ (1392.09): calcd. C 34.51, H 4.63, N 21.13; found C 34.27, H 4.72, N 21.33. UV/Vis (MeOH/MeCN, 9:1 v:v): λ_{max} (ε) = 228 sh (22600), 276 (4500), 402 (4500), 644 nm (542 M^{-1} cm^{-1}). CD (MeOH/MeCN, 9:1 v:v): λ_{max} ($\Delta\varepsilon$) = 250 sh (+2.22), 274 (+ 2.71), 380 (+ 2.08), 438 (–1.69), 498 (–0.46), 525 (–0.57), 620 nm (+1.08 M^{-1} cm^{-1}).

Azide Binding Studies: The binding of azide to [Cu$_2$PHI][ClO$_4$]$_4$ and [Cu$_3$PHI][ClO$_4$]$_6$ was studied spectrophotometrically by adding concentrated methanolic solutions of sodium azide to solutions of the complexes dissolved in MeOH/MeCN, 9:1 (v/v). All measurements were performed in a thermostatted optical cell, with magnetic stirring, at 20 ± 0.1 °C. In all cases, it was found that binding of the anion is fast, so it was not necessary to incubate the mixtures before the spectroscopic measurements were performed. Titration of [Cu$_2$PHI]$^{4+}$ (2.78 × 10^{-4} M) was performed by the addition of successive and equal amounts of an azide solution (2.40 × 10^{-3} M) from 0.1 to 2.0 [azide]:[Cu$_2$] unitary ratios. Further addition of azide did not produce appreciable spectral changes. It was possible to separate the titration steps for [N$_3$$^-$]:[Cu$_2$] between 0.1 and 1 ($\lambda_{max}$ = 396 nm, isosbestic point at 340 nm) and between 1.1 to 2.0 (λ_{max} = 396 nm, isosbestic point at 348 nm). In a similar way, titration of [Cu$_3$PHI]$^{6+}$ (2.54 × 10^{-4} M) was carried out by the stepwise addition of 0.1 molar equiv. of azide (from a 2.40 × 10^{-3} M solution) between a 0.1 to 2.0 [N$_3$$^-$]:[Cu$_3$] ratio, and then 0.2 molar equiv. of azide from a 2.2 to 3.0 [N$_3$$^-$]:[Cu$_3$] ratio. In this case, though, it was not possible to separate the various steps of the titration. In order to determine the binding constants and stoichiometry of the formation of the adducts, the spectroscopic data were analyzed as described previously.[10]

Synthesis of [Cu$_3$PHI][PF$_6$]$_3$: Solid [Cu(CH$_3$CN)$_4$](PF$_6$) (33 mg, 9.0 × 10^{-2} mmol) was added to a solution of the ligand PHI (25 mg, 3.0 × 10^{-2} mmol) in dry CH$_2$Cl$_2$ (8 mL) whilst stirring and kept under an inert atmosphere. The solution was stirred for about 20 min and then concentrated under reduced pressure. The white precipitate of the Cu^I complex was collected by filtration, washed with a small amount of diethyl ether and then carefully dried under vacuum (yield 75%). The extreme oxygen sensitivity of this copper(I) complex prevented any spectroscopic characterization from being performed.

Attempted Oxygenation of [Cu$_3$PHI][PF$_6$]$_3$: A chilled concentrated solution of [Cu$_3$PHI][PF$_6$]$_3$ in acetone was transferred under Ar into anhydrous CH$_2$Cl$_2$ (25 mL) thermostatted at –78 °C (final concentration of the Cu^I complex 1.6 × 10^{-4} M). Dry oxygen was then bubbled through the solution for about 20 min, without observing an evident change in the color of the solution.

Hydroxylation of *p*-Chlorophenolate: A solution of the complex [Cu$_3$PHI][PF$_6$]$_3$ (4.0 × 10^{-3} mmol) in anhydrous CH$_2$Cl$_2$ (25 mL) was treated with O$_2$ (1 atm) at –78 °C for 30 min. A cooled solution of sodium *p*-chlorophenolate (4.0 × 10^{-3} mmol) in dry CH$_2$Cl$_2$ (1 mL) was then added with a syringe. After 30 min, the reaction mixture was quenched by the addition of 0.4 M HClO$_4$ (3 mL) and the solvent was removed under vacuum until the residual volume was about 3 mL. The residual solution was treated with CH$_2$Cl$_2$ (20 mL) and the organic phase was washed three times with a small amount of aqueous HClO$_4$ and water, and it was then taken to dryness under reduced pressure. The residue was treated with 2 mL of a 1:1 mixture of MeCN/water. The solutions were then analyzed by HPLC using a Supelco LC18 semipreparative column (250 × 10 mm). Elution was carried out using 0.1% TFA in distilled water (solvent A) and 0.1% TFA in acetonitrile (solvent B), with a flow rate of 5.0 mL/min. The elution started with 80% solvent A for 5 min, over the next 50 min the eluting solvent was brought to

0% A, then kept constant for an additional 5 min, and finally returned to 80% A over 5 min. The HPLC analysis shows that the only detectable product is the catechol derived from *p*-chlorophenol. In fact, the HPLC chromatograms of the mixtures obtained from oxygenation experiments contained only three peaks: *p*-chlorocatechol (11.8 min elution time), unreacted *p*-chlorophenol (16.5 min), and traces of the ligand (6.0 min). Samples of the HPLC peak eluting at 11.8 min from five HPLC runs were collected and the solvent was rotary evaporated. The residue was treated with 0.75 mL of CD_3CN and a ^1H NMR spectrum was recorded, confirming the presence of *p*-chlorocatechol. Quantification of the catechol in the reaction mixtures was performed by HPLC using *p*-cyanophenol as an internal standard (7.28 min retention time).

[Zn₃PHI][ClO₄]₆: The complex [Zn₃PHI][ClO₄]₆ was prepared in situ by adding solid $Zn(ClO_4)_2 \cdot 7H_2O$ (0.06 mmol) to a [D₆]acetone solution (0.5 mL) of the ligand PHI (0.018 mmol). The solution was gently stirred for 2 h at room temperature and then used as such for the NMR spectroscopic experiments.

Supporting Information (see also the footnote on the first page of this article): Simulation of the X-band EPR spectra for the Cu^{II} ions in the two binding sites of the PHI molecule (Figure 1S), and complete NMR spectroscopic data for PHI (Figure 2S) and [Zn₃PHI]⁶⁺ (Figure 3S).

[1] a) K. D. Karlin, *Science* **1993**, *261*, 701–708; b) J. Reedijk, E. Bowman, *Bioinorganic Catalysis*, 2nd ed., Marcel Dekker, New York, **1999**; c) J. DuBois, T. J. Mizoguchi, S. J. Lippard, *Coord. Chem. Rev.* **2000**, *200–202*, 443–485.

[2] a) E. A. Lewis, W. B. Tolman, *Chem. Rev.* **2004**, *104*, 1047–1076; b) L. Q. Hatcher, K. D. Karlin, *Adv. Inorg. Chem.* **2006**, *58*, 131–184; c) L. M. Mirica, X. Ottenwaelder, T. D. P. Stack, *Chem. Rev.* **2004**, *104*, 1013–1045; d) G. Battaini, A. Granata, E. Monzani, M. Gullotti, L. Casella, *Adv. Inorg. Chem.* **2006**, *58*, 185–233; e) S. Itoh, S. Fukuzumi, *Acc. Chem. Res.* **2007**, *40*, 592–600.

[3] P. Gamez, P. G. Aubel, W. L. Driessen, J. Reedijk, *Chem. Soc. Rev.* **2001**, *30*, 376–385.

[4] a) E. I. Solomon, R. Sarangi, J. S. Woertink, A. J. Augustine, J. Yoon, S. Ghosh, *Acc. Chem. Res.* **2007**, *40*, 581–591; b) T. Bertrand, C. Jolivalt, P. Briozzo, E. Caminade, N. Joli, C. Madzak, C. Mougin, *Biochemistry* **2002**, *41*, 7325–7333; c) I. Bento, L. O. Martins, G. C. Lopes, M. A. Carrondo, P. F. Lindsey, *Dalton Trans.* **2005**, 3507–3513.

[5] a) M. C. Mimmi, M. Gullotti, L. Santagostini, A. Saladino, L. Casella, E. Monzani, R. Pagliarin, *J. Mol. Catal. A* **2003**, *204–205*, 381–389; b) M. C. Mimmi, M. Gullotti, L. Santagostini, R. Pagliarin, L. De Gioia, E. Monzani, L. Casella, *Eur. J. Inorg. Chem.* **2003**, 3934–3944; c) M. C. Mimmi, M. Gullotti, L. Santagostini, L. Casella, G. Battaini, E. Monzani, R. Pagliarin, G. Zoppellaro, *Dalton Trans.* **2004**, 2192–2201; d) M. Gullotti, L. Santagostini, R. Pagliarin, A. Granata, L. Casella, *J. Mol. Cat. A Chem.* **2005**, *235*, 271–284.

[6] L. Santagostini, M. Gullotti, R. Pagliarin, E. Bianchi, L. Casella, E. Monzani, *Tetrahedron: Asymmetry* **1999**, *10*, 281–295.

[7] L. Santagostini, M. Gullotti, R. Pagliarin, E. Monzani, L. Casella, *Chem. Commun.* **2003**, 2186–2187.

[8] S. F. Mason, *Molecular Optical Activity and the Chiral Discrimination*, Cambridge University Press, Cambridge (UK), **1982**.

[9] L. Casella, M. Gullotti, G. Pallanza, M. Buga, *Inorg. Chem.* **1991**, *30*, 221–227.

[10] L. Casella, O. Carugo, M. Gullotti, S. Garofani, P. Zanello, *Inorg. Chem.* **1993**, *32*, 2056–2067.

[11] J. E. Pate, P. K. Ross, T. J. Thamann, C. A. Reed, K. D. Karlin, N. T. Sorrell, E. I. Solomon, *J. Am. Chem. Soc.* **1989**, *111*, 5198–5205.

[12] L. Casella, O. Carugo, M. Gullotti, S. Doldi, M. Frassoni, *Inorg. Chem.* **1996**, *35*, 1101–1113.

[13] a) H. P. Jensen, E. Larsen, *Acta Chem. Scand.* **1971**, *25*, 1439–1451; b) L. Casella, M. Gullotti, R. Pagliarin, M. Sisti, *J. Chem. Soc., Dalton Trans.* **1991**, 2527–2531.

[14] a) S. Itoh, H. Kumei, M. Taki, S. Nagatomo, T. Kitagawa, S. Fukuzumi, *J. Am. Chem. Soc.* **2001**, *123*, 6708–6709; b) L. Santagostini, M. Gullotti, E. Monzani, L. Casella, R. Dillinger, F. Tuczek, *Chem. Eur. J.* **2000**, *6*, 519–522; c) S. Palavicini, A. Granata, E. Monzani, L. Casella, *J. Am. Chem. Soc.* **2005**, *127*, 18031–18036; d) L. M. Mirica, M. Vance, D. J. Rudd, B. Hedman, K. O. Hodgson, E. I. Solomon, T. D. P. Stack, *Science* **2005**, *308*, 1890–1892; e) L. M. Mirica, D. J. Rudd, M. A. Vance, E. I. Solomon, K. O. Hodgson, B. Hedman, T. D. P. Stack, *J. Am. Chem. Soc.* **2006**, *128*, 2654–2665.